

Figure 1 Typical microlens array for Shack-Hartmann Sensor (S: Pitch between neighboring microlenses, G_L : Gap between neighboring microlenses, D_L : Diameter of microlenses, Numbers in blue: Identification numbers assigned to microlenses)

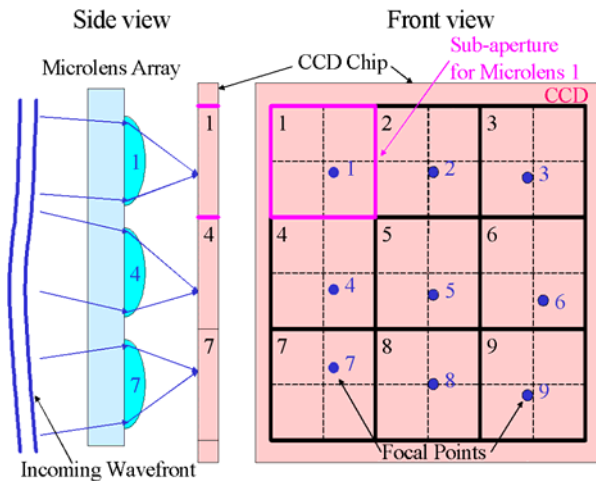


Figure 2 Wavefront slope measurement using microlens array: Each microlens has its own sub-aperture consisted of four CCD pixels, and the focal point of the microlens must be located within the assigned sub-aperture.

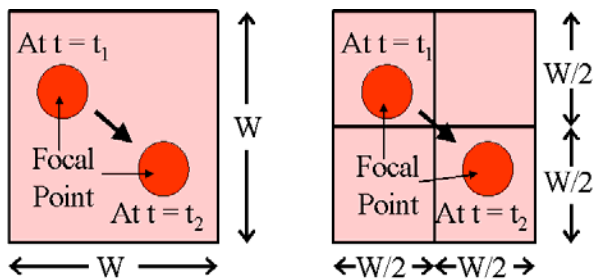


Figure 3 Advantage of having smaller pixels: CCD with larger pixels (left) cannot detect the shift in position of the focal spot while CCD with smaller pixels (right) can easily detect the change.

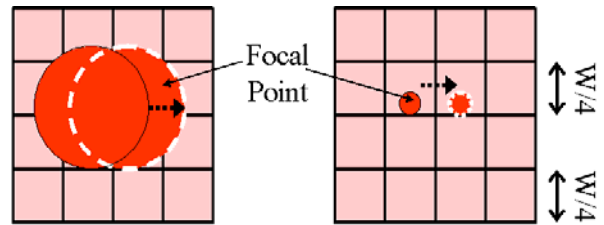


Figure 4 Advantage of having smaller focal spot on CCD with super-fine pixels: Larger focal point compromises the sensitivity, spatial resolution, and accuracy.

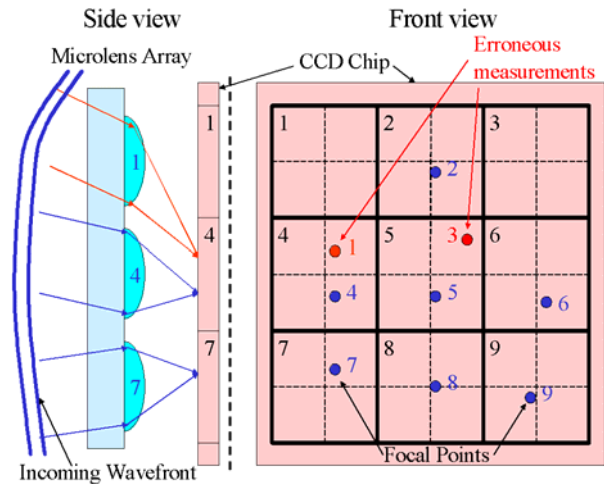


Figure 5 Dislocation of focal points due to large curvature of the wavefront: The focal points of microlens #1 and #3 are dislocated onto the sub-apertures assigned to microlens #4 and #5, respectively, causing erroneous measurements.

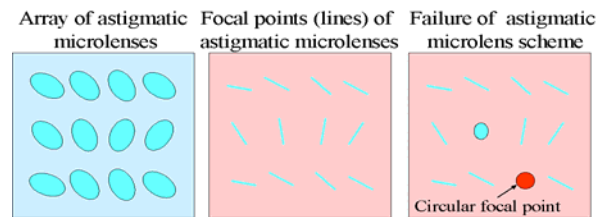


Figure 6 Dynamic range expansion using astigmatic microlenses and its failure: Once the focal point becomes circular, its origin cannot be traced.

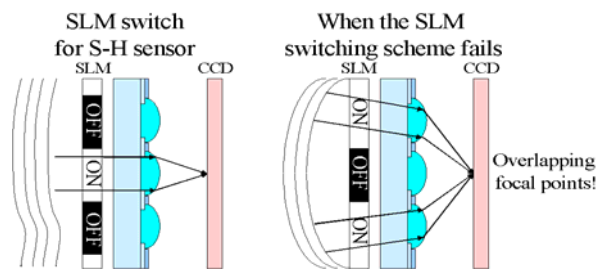
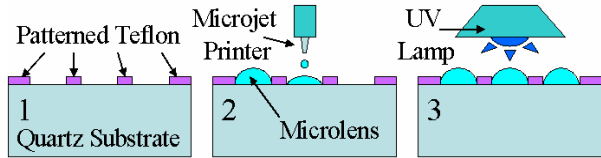


Figure 7 Dynamic range expansion of Shack-Hartmann sensor using a spatial-light modulator



1. Spin-coat a 0.2 μm thick Teflon (hydrophobic) layer on quartz wafer. Then, photolithographically pattern and dry-etch the Teflon layer using low power O_2 plasma.
2. Using the inkjet print head, dispense the desired amount of UV-curable polymer within the hydrophilic circles.
3. Fully cure the polymer lens under a high-intensity UV lamp.

Figure 8 Fabrication Process:

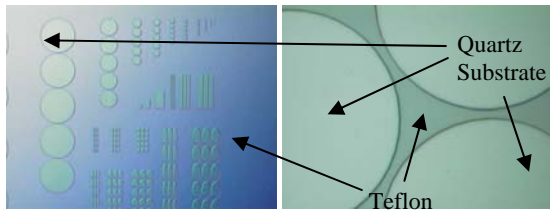


Figure 9 Various hydrophilic patterns created on a hydrophobic Teflon layer on quartz substrate

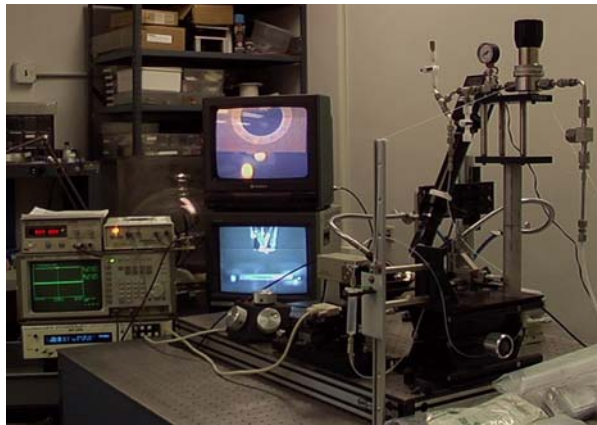


Figure 10(a) Fabrication setup: Microjet printer and driver, automated stage, and viewing system.

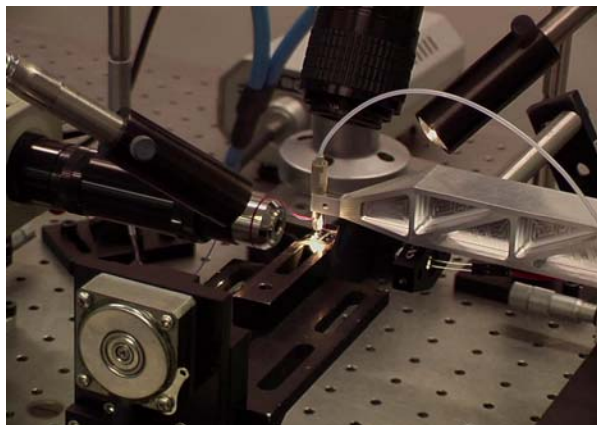


Figure 10(b) Enlarged view of microjet printer, automated stage, and viewing system

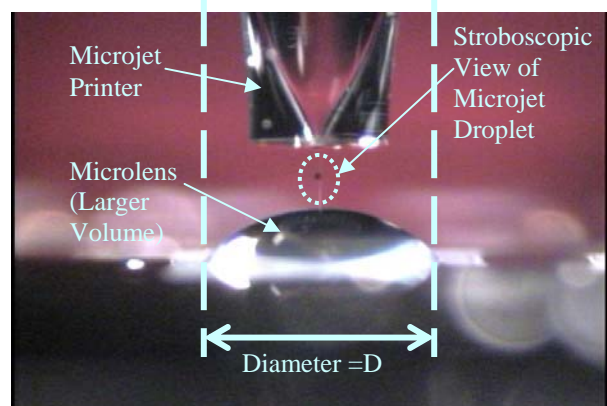
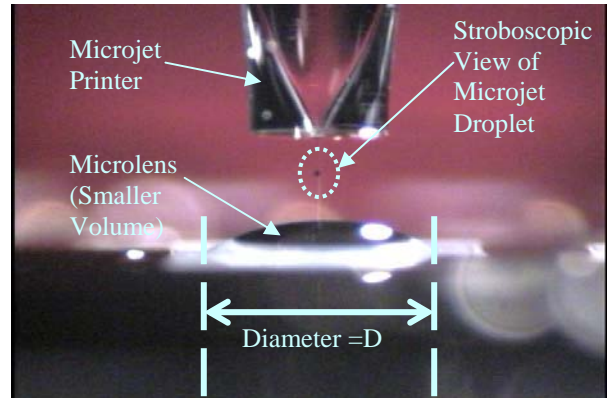


Figure 11 Controlling the curvature of 1000 μm -diameter microlens: Change in volume clearly changes the curvature/height of the microlens for a given diameter.

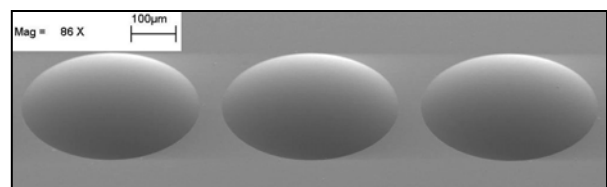


Figure 12 Uniform 400 μm -diameter microlenses



Figure 13 Variation of microlens curvatures for 400- μm diameter

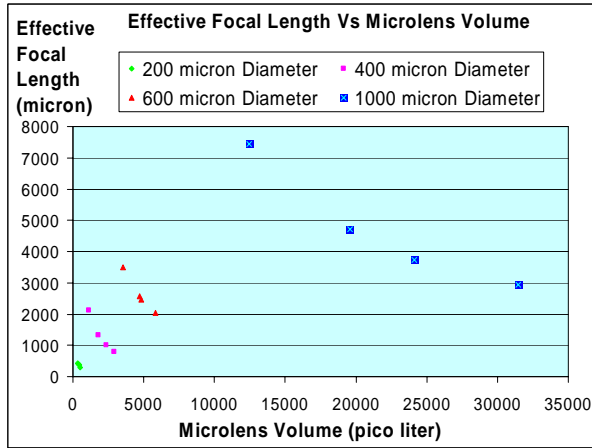


Figure 14 Effective focal length Vs microlens volume

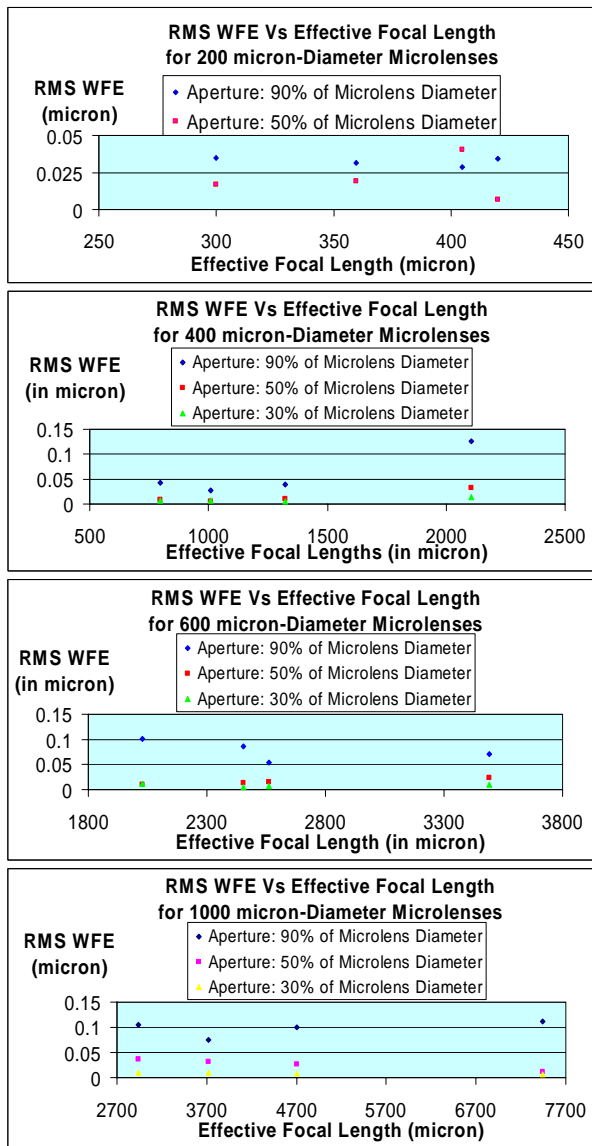


Figure 15 Rms wavefront error Vs effective focal length for various microlenses

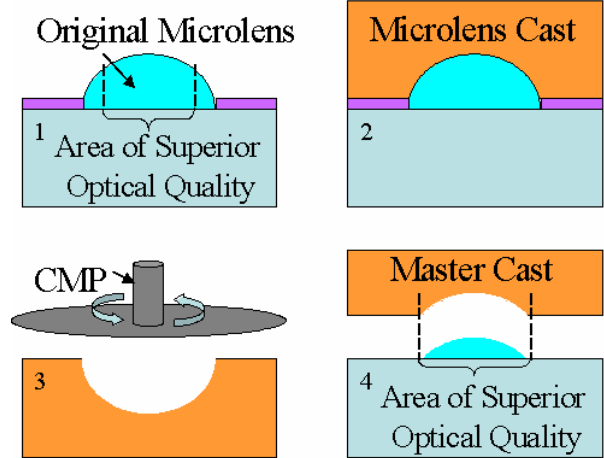


Figure 16 Producing a master element for high-precision microlens replication

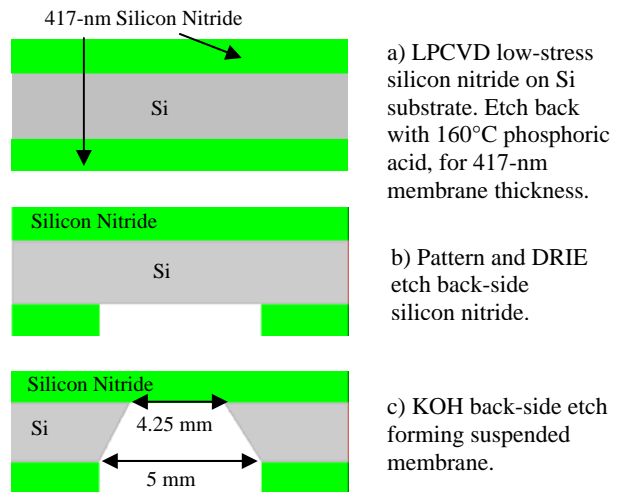


Figure 17 Beam splitter process flow

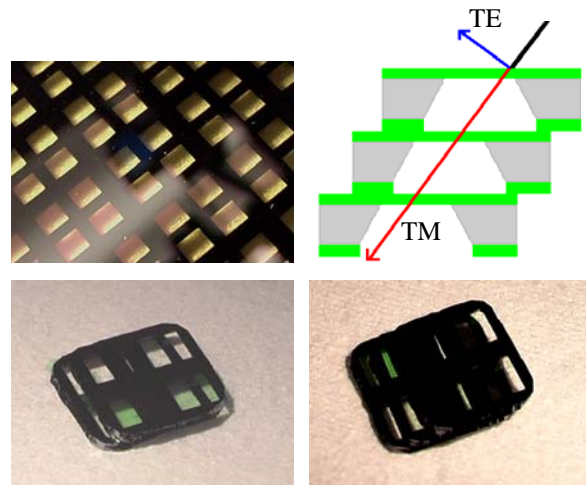


Figure 18 Single-, double-, triple-nitride membrane PBS

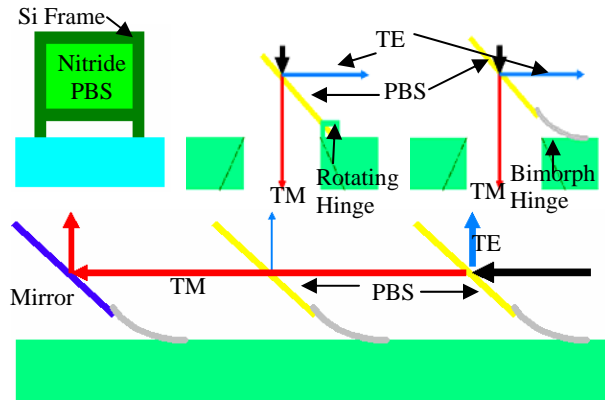


Figure 19 Possible integration schemes for the multi-layer PBS with MEMS structures

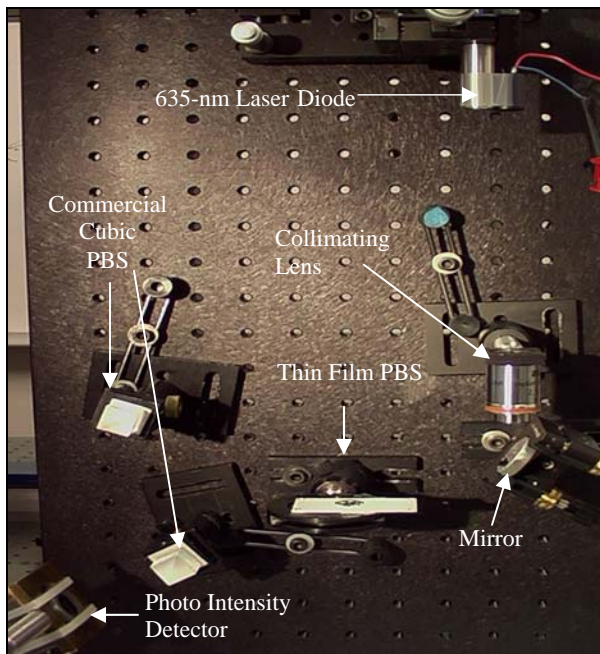


Figure 20 Optical testing setup for thin-film PBS

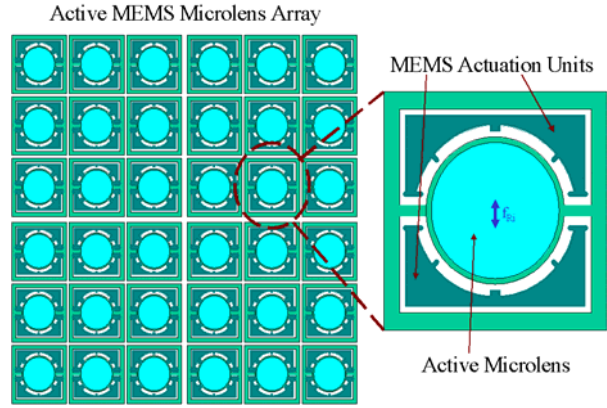


Figure 21 Schematic diagram of active MEMS microlens array and enlarged view of individually active microlens unit

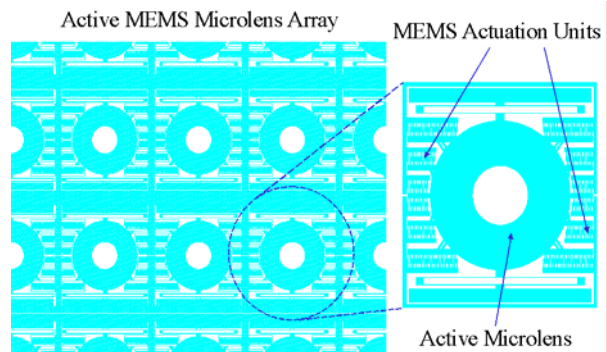
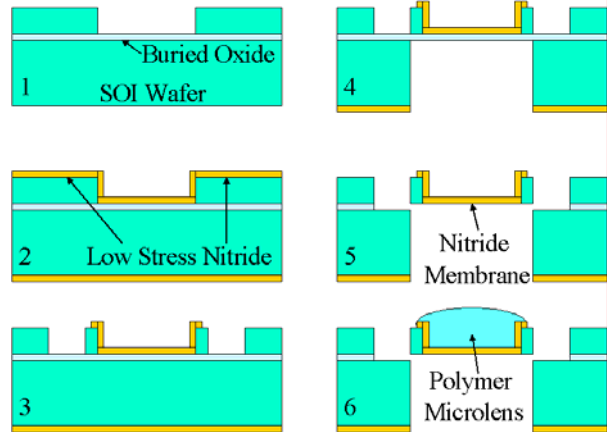


Figure 22 Actual layout of our prototype active MEMS microlens array and enlarged view of individually active microlens unit



1. RIE the device layer to create an opening for microlens.
2. Deposit LPCVD low stress nitride layer.
3. Pattern the nitride layer and RIE the device layer to create MEMS actuators.
4. RIE the handling layer to create an opening for microlens.
5. Release the structure in 49% concentrated HF.
6. Make microlens using our Polymer-Jet printer.

Figure 23 Fabrication Process for active MEMS microlens array:

Table 1 Reflected and transmitted light extinction ratios for single-, double-, and triple-nitride membranes

	Single-Layer PBS*	Double-Layer Stacked PBS	Triple-Layer Stacked PBS
Insertion Loss	3%	10%	13%
Reflected _{TE} / Reflected _{TM}	99.2%	99.2%	99.2%
Transmitted _{TM} / Transmitted _{TE}	90.9%	96.2%	97.5%
Reflected Light Extinction Ratio (dB)	21	21	21
Transmitted Light Extinction Ratio (dB)	10	14	16
Film Thickness Layer 1 (nm)	419.3	419.5	419.5
Film Thickness Layer 2 (nm)	N/A	419.2	419.2
Film Thickness Layer 3 (nm)	N/A	N/A	419.5

* Average values for 10 different single-layer structures